

LABORATORY EVALUATION ON PERFORMANCE OF GLASS FIBER REINFORCED PLASTIC MORTAR PIPE CULVERTS

Huawang Shi^{1,2}, Lianyu Wei³

- 1. Hebei University of Technology, School of Civil Engineering, Tianjin, China; e-mail:stone21st@163.com*
- 2. Hebei University of Engineering School of Civil Engineering, Handan, China; email:stone21st@163.com*
- 3. Hebei University of Technology, School of Civil Engineering, Tianjin, China; e-mail:shw2016@sohu.com*

ABSTRACT

This paper investigated the performance and behaviour of glass fiber reinforced plastic mortar (FRPM) pipes under different loading conditions. FRPM pipes with inner diameter of 1500 mm were prefabricated in factory. Mechanics performance testing (ring and axial compressive strength and elastic modulus), stiffness and fatigue test were carried out in laboratory. Ring stiffness test provided pipe stiffness (PS) which is a function of geometry and material type of pipe through parallel plate loading test (PPLT). The fatigue test and micro-structure measure method were used to evaluate the durability effects of FRPM under repeated compression load. Results indicated that FRPM pipes had better mechanic performances as the road culverts under soils. It may be helpful for the design and construction of FRPM culverts.

KEYWORDS

Mechanic performances, FRPM, Ring stiffness, Fatigue

INTRODUCTION

Glass fiber reinforced plastic mortar (FRPM) pipe is a kind of new composite material using resin as matrix material, glass fiber and its products as reinforced material, and quartz sand as filling material. According to the production process, it can be divided into three categories named fixed-length winding, centrifugal casting and continuous winding. Due to the excellent corrosion resistance, good bearing capacity, small internal resistance, long service life, easy installation, rapid construction time and lower initial and long-term maintenance costs, FRPM pipes have been widely used in road engineering.

As an important part of highway engineering, culverts make up a significant proportion of all road projects both on the quantity and the project cost. FRPM pipes arising in the 1970s were always used as a flexible composite pipe. FRPM pipeline was made initially from 1979 in Italy, and then spread to China, European and African countries. By 1992, all kinds of FRPM pipelines used as sewage pipe, fire hose, water and waste water pipe had reached 1020 km in Italy, from 200 to 3050 mm in diameter. FRPM pipelines with large diameter accounted for about 40%. The pipes used in Spain, Monaco, Nigeria, the united Arab emirates, Saudi Arabia, Iran and other countries, are about 400 km. In 1979, sand glass fiber reinforced plastic pipeline was made in Italy, successively used in China, European and African countries. Rafiee and Amini (2015) performed

the study of failure mechanism of FRPM, developed the continuous failure damage model (SFM), and verified it through the different layer structure of mechanical properties of FRPM test. Ouellette and Beach (1981) studied the design method of FRPM pipeline, suggested that based on the structural feature of FRPM and load requirements, the maximum load, flexural strength, shear strength and the bearing capacity of each layer must be calculated. Sung and Jin (2015) predicted the long-term performance of FRPM pipe under continuous internal pressure. According to the data of the continuous internal pressure test, they found that the linear regression analysis is suitable to predict the failure pressure of FRPM after 50 years. Rafiee and Reshadi (2014) observed the GRP tube under hydrostatic pressure and found that the first fracture (FPF) and the functional failure (FF) pressure increased linearly with the core thickness increasing. Xia, etc. (2001) investigated the mechanical properties of composite pipes under internal pressure. The stress-strain relationship was obtained. At the same time, they pointed out that the axial tensile stiffness of the inner surface of the pipeline was larger than that of the outer surface.

Through investigation of FRPM pipe in service, we found many FRPM pipes with disease, due to the existing design and construction method. The deformation and stress characteristics of culvert structure under loads of filled soil are still not very clear. Therefore enough guidelines for design and construction were not provided. For the former problems of FRP pipes in highway bridge engineering application, both in terms of design standard and mechanics analysis, or in the construction process and quality control on test methods and standards, still need to conduct more in-depth theoretical and applied basic research work, to guide the application of FRP pipes in highway bridge engineering before has good prospects for development.

MATERIALS AND METHODS

FRPM Pipes Description

Glass fiber used here is a kind of improved glass without boron and alkali, ECR roving - 2400-906, produced by Jiangsu composite materials co. LTD. As shown in Figure 1 (a), it can be used in the production of acid and water resistance glass fiber, and it is one of the new materials designed for underground pipe, tank and so on. The glass fiber surface mat refers to the glass fiber reinforced plastic products which can form resin layer. It is typically implemented with the alkali glass surface mat (Figure 1 (b)). Glass fiber stitched mat (Figure1(c)) is available to sew it into the short cut fiber or long fiber by using stitched knitting machine.



(a) Glass fiber



(b) Glass fiber surface mat



(c) Glass fiber stitched mat

Fig. 1 - Glass fiber production

Resin is DM - 196 unsaturated polyester resin produced with Shandong Texas plains new Dongming resin co. LTD. Its physical, chemical and mechanical properties are listed in Table 1.

The mort used is quartz sands that generally selected to remove dust or other debris in the drying process. The following technical indicators are presented in Table 2.

Tab. 1 - Unsaturated polyester resin

| Appearance | Type | viscosity /cp.25°C | Distortion temperature /°C | Tensile strength /MPa | Breaking elongation /% |
|------------|---------------|--------------------|----------------------------|-----------------------|------------------------|
| Reseda | Orthophthalic | 400 | 70 | 65 | 3 |

Tab. 2 - Physical and chemical indicators

| Physical indicators | | | | Chemical indicators | | |
|-------------------------|-------------------|-------|--|---------------------|-------|--|
| Indicator | Unit | Value | Indicator | Unit | Value | |
| Proportion | g/cm ³ | 2.66 | SiO ₂ | % | 99 | |
| Unit weight | g/cm ³ | 1.75 | Hydrochloric acid soluble rate | % | 3.0 | |
| Fracturing propane | % | 0.53 | Acid fastness | % | 98 | |
| Coefficient of friction | % | 0.35 | Melting point | °C | 1480 | |
| Porosity | % | 43~47 | Boiling point | °C | 2550 | |
| Moh's hardness | | 7.5 | Ca | % | 0.02 | |
| Sediment percentage | % | 1 | Zn | % | 0.005 | |
| Non-uniform coefficient | k80 | 1.8 | All indexes meeting to CJ/T43-2005 standards | | | |

Mechanical properties of FRPM test

In order to obtain the ring and axial compressive strength and elastic modulus through the indoor test, the samples were divided into two types including ring and axial direction specimen, and two mechanical indexes consisting of compressive strength and elastic modulus were measured for each type of samples. Test equipment was computer control electro-hydraulic servo universal testing machine (WAW - 1000 system), as shown in Figure 2. Electronic gauge is used to measure the displacement.



Fig. 2 - Laboratory test system

According to the data of laboratory test, the compressive strength and elastic modulus can be obtained by the following calculation method. Roy and Tsai. (2012) calculated the compressive strength of FRPM pipe by:

$$\sigma_c = \frac{P}{a \times b} \tag{1}$$

where: σ_c is the Compressive strength (kN/cm²) ;

P is the Ultimate load (kN) ;

a,b are length and width of the sample (cm) .

According to the Equation 1, we can calculate the elastic modulus:

$$E_c = \frac{L \cdot \Delta P}{a \cdot b \cdot \Delta L} \quad (2)$$

where: E_c is the Elasticity modulus;

ΔP is the Load increment;

ΔL is the Deformation increment corresponding to ΔP ;

L is the Thickness of the sample.

Pipe stiffness of FRPM test

Pipe stiffness refers to the bearing force that unit length of pipe under loads and at certain radial deformation. Pipe stiffness expressing characterization ability of pipeline resists external load is shown in Figure 3. Pipe stiffness is the key parameter in the process of municipal pipeline design. This experiment through parallel plate load is to test FRPM pipe's ability to resist deformation, analyse FRPM pipe's stiffness and the relationship between force and deformation curve under the external load (Qi H Y, Wen W D., 2001). Considering the actual testing is often done under deformation rate is less than 3%, this type formula can be written as:

$$PS = 0.01935 \frac{F}{\Delta Y} \quad (3)$$

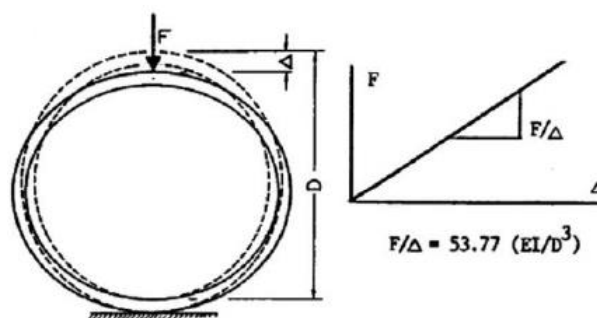


Fig. 3 - Parallel plate performance testing under external load

Tensile Fatigue Test

Fatigue property of FRPM pipe is closely related to the service life of FRPM culvert. The better the fatigue property of FRPM pipe is, the longer the service life of culvert. Thereby, it is necessary to investigate the fatigue property of FRPM pipe (Xu, WenW and Cui, 2006; Guo and Bian et.,2015).There are many factors affecting the fatigue performance such as the size of the sand in stratified layer, material properties of different layers, stress history, testing stress, stress amplitude, test environment, etc., and the influence degree of various factors on the fatigue performance are unclear. Therefore, in order to eliminate the influence of material properties on the

test results, the FRPM pipes with the same manufacturer and batch products were used in this test. The specimens used in this experiment were uniform in the wall thickness, and the diameter was 1.5 m, thickness 50 mm and 300 mm long. Constant amplitude fatigue test (CAFT) is an effective method which has been used in many researches, so this method was used to investigate the fatigue property of FRPM pipe.

The representative test procedure was shown in Figure 4.

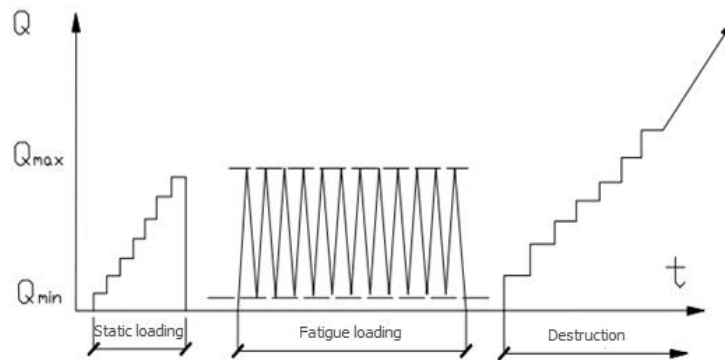


Fig. 4 - Fatigue test procedure

Constant amplitude fatigue test was performed by the MTS loading fatigue testing machine, as shown in Figure 5 and Figure 6.



Fig. 5 - Test loading system

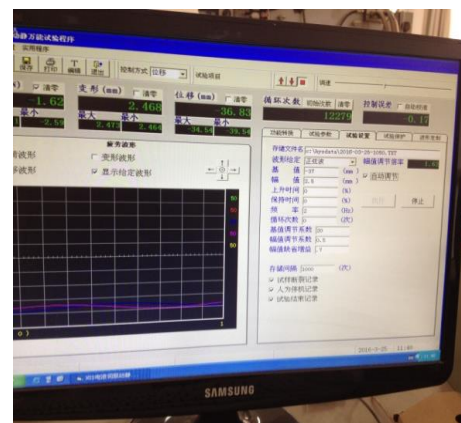


Fig. 6 - Test data acquisition system

This test was conducted at a room temperature, 23.5°C. A stress-control mode was applied. As shown in Figure 4, this method is characterized as:

$$r = 0, S_{\min} = 0, S_m = S_a = \frac{1}{2} S_{\max}$$

where, $S_{\max 1} = 4.12 \text{ kN}$, $S_{\max 2} = 7.1 \text{ kN}$. In the process of fatigue test, respectively in cyclic times to: 10000 times, 500000 times, 1 million times, 1.5 million times, 2 million times Equipment downtime due to a static load test. The static load test was carried out with five times of loading and unloading.

RESULTS

Compressive resistance of FRPM

Compressive resistance results were obtained by compressive test. Figure 7 shows the relationship between the displacement and the force of compression strength test. In Figure 7, it can be observed that, from the beginning of the displacement 2.660mm, the force specimen bearing at all measuring points are continuously increased. However, after reaching the peak force of 127.89kN, the curve of graph decreased significantly. Figure 8 shows the destruction sample after compressive strength test.

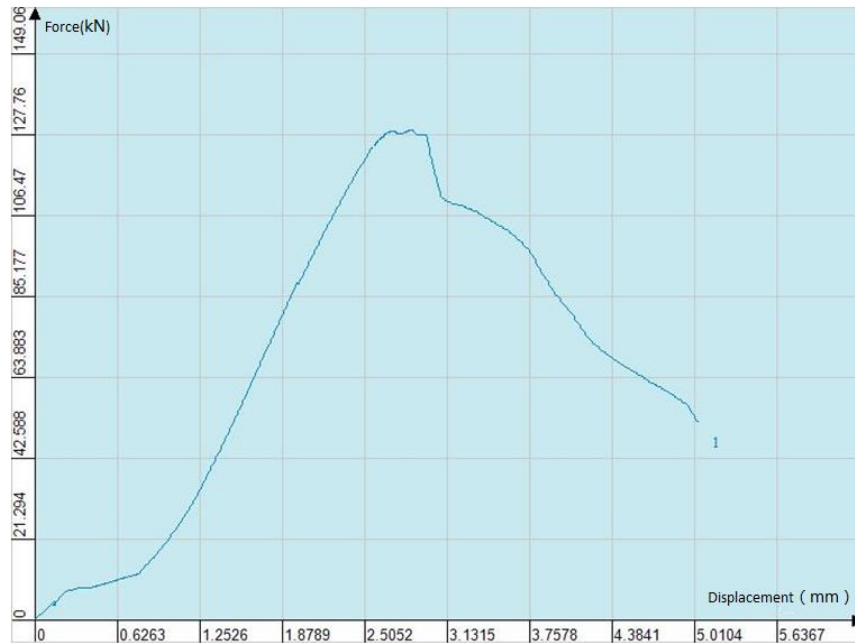


Fig. 7 - Typical curve of compressive strength testing



Fig. 8 - Ring and axial sample destruction form

After determination of limit bearing capacity of FRPM, elastic modulus experiment was carried out with the maximum load is 50% of the ultimate compressive load. The circular and axial elastic modulus is shown in Table 3 and Table 4. From Table 3 and Table 4, we can conclude that the ring and axial elastic module of FRPM are 4.84GPa and 3.04GPa respectively.

Tab. 3 - Ring elasticity modulus

| Test specimen | Test data | | | | | | | | Elasticity modulus E (GPa) |
|----------------------------|------------------|-------|-------|-------|-------|-------|-------|-------|-------------------------------|
| HY1 | Load (kN) | 5 | 10 | 15 | 20 | 25 | 30 | 35 | 4.39 |
| | Deformation (mm) | 0.095 | 0.171 | 0.244 | 0.314 | 0.385 | 0.450 | 0.532 | |
| HY2 | Load (kN) | 5 | 10 | 15 | 20 | 25 | 30 | 35 | 5.96 |
| | Deformation (mm) | 0.082 | 0.140 | 0.191 | 0.228 | 0.295 | 0.347 | 0.400 | |
| HY3 | Load (kN) | 5 | 10 | 15 | 20 | 25 | 30 | 35 | 4.64 |
| | Deformation (mm) | 0.110 | 0.172 | 0.244 | 0.309 | 0.380 | 0.444 | 0.504 | |
| HY4 | Load (kN) | 5 | 10 | 15 | 20 | 25 | 30 | 35 | 4.50 |
| | Deformation (mm) | 0.120 | 0.196 | 0.271 | 0.340 | 0.400 | 0.468 | 0.529 | |
| HY5 | Load (kN) | 5 | 10 | 15 | 20 | 25 | 30 | 35 | 4.70 |
| | Deformation (mm) | 0.083 | 0.151 | 0.217 | 0.279 | 0.350 | 0.415 | 0.476 | |
| Mean elastic modulus (GPa) | | | | | | | | 4.84 | |

Tab. 4 - Axial elastic modulus

| Test specimen | Test data | | | | | | | | Elasticity modulus E (GPa) |
|----------------------------|------------------|-------|-------|-------|-------|-------|-------|-------|-------------------------------|
| ZY1 | Load (kN) | 5 | 10 | 15 | 20 | 25 | 30 | 35 | 2.74 |
| | Deformation (mm) | 0.130 | 0.251 | 0.356 | 0.468 | 0.570 | 0.697 | 0.823 | |
| ZY2 | Load (kN) | 5 | 10 | 15 | 20 | 25 | 30 | 35 | 3.14 |
| | Deformation (mm) | 0.157 | 0.279 | 0.381 | 0.472 | 0.571 | 0.670 | 0.763 | |
| ZY3 | Load (kN) | 5 | 10 | 15 | 20 | 25 | 30 | 35 | 3.04 |
| | Deformation (mm) | 0.117 | 0.220 | 0.320 | 0.415 | 0.510 | 0.626 | 0.730 | |
| ZY4 | Load (kN) | 5 | 10 | 15 | 20 | 25 | 30 | 35 | 3.05 |
| | Deformation (mm) | 0.123 | 0.211 | 0.306 | 0.406 | 0.511 | 0.622 | 0.728 | |
| ZY5 | Load (kN) | 5 | 10 | 15 | 20 | 25 | 30 | 35 | 3.24 |
| | Deformation (mm) | 0.106 | 0.194 | 0.279 | 0.375 | 0.473 | 0.571 | 0.684 | |
| Mean elastic modulus (GPa) | | | | | | | | 3.04 | |

Pipe stiffness (PS) of FRPM

Though parallel plate performance test under external load, the load - deformation data shown in Figure 9 were obtained. According to Equation 3, pipe stiffness (PS) is 2.3 MPa, and stiffness factor (SF) is 2.8kPa·m³.

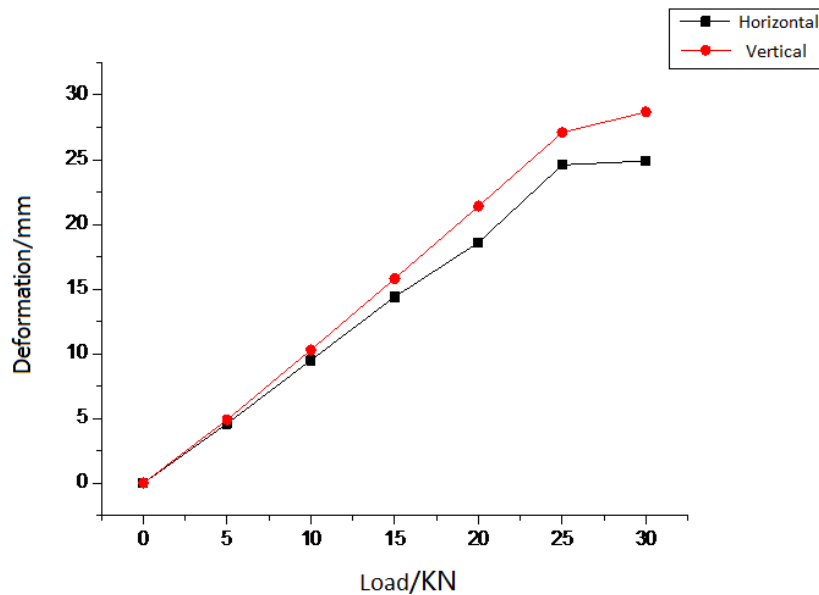


Fig. 9 - Load – deformation curve

Fatigue performance of FRPM

Table 5 and Table 6 reflect deflection increment- load data of GH1 and GH2 after different cycles of fatigue load respectively. If the specimens have not damaged after 2 million times of fatigue loading, downtime for static load, we can obtain the ultimate bearing capacity as shown in Figure 10. Experiencing 2 million fatigue loads, FRPM produce the maximum crack width of 1.85 mm at failure stage, and directly maximum crack width is 3.87 mm did not experience fatigue load, as shown in Figure 11. The fatigue crack width is obviously smaller than the crack width without fatigue loading. Thus, due to the development of internal defects after the fatigue loading of FRPM, stiffness and bearing capacity of FRPM is falling, but due to the internal microstructure changing and restructuring, the failure form of FRPM trends from brittle to plastic(Farshad and Necola.,2004).

Tab. 5 - Deflection increment- load data of GH1

| Displacement /mm | 0.1million Load/kN | 0.5million Load /kN | 1 million Load /kN | 1.5 million Load /kN | 2 million Load /kN |
|------------------|--------------------|---------------------|--------------------|----------------------|--------------------|
| 0 | 0 | -0.06 | 0 | -0.14 | 0 |
| 2 | 3.9 | -0.83 | -0.9 | -1 | -0.89 |
| 4 | 4.5 | -1.58 | -1.72 | -1.82 | -1.67 |
| 6 | 6.3 | -2.37 | -2.57 | -2.65 | -2.5 |
| 8 | 8.3 | -3.18 | -3.35 | -3.42 | -3.29 |
| 10 | 10.2 | -3.97 | -4.15 | -4.16 | -4.03 |
| 12 | 12 | -4.75 | -4.9 | -4.91 | -4.75 |
| 14 | 12.8 | -5.45 | -5.66 | -5.64 | -5.49 |
| 16 | 14 | -6.2 | -6.37 | -6.34 | -6.22 |
| 18 | 16 | -6.94 | -7.16 | -7.08 | -6.96 |
| 20 | 17.8 | -7.7 | -7.9 | -7.86 | -7.72 |
| 22 | 18 | -8.46 | -8.71 | -8.62 | -8.45 |
| 24 | 19.8 | -9.2 | -9.45 | -9.34 | -9 |

| | | | | | |
|----|------|--------|--------|--------|--------|
| 26 | 21 | -9.93 | -10.2 | -10.05 | -9.86 |
| 28 | 22.2 | -10.64 | -10.88 | -10.78 | -10.58 |
| 30 | 24 | -11.34 | -11.68 | -11.5 | -11.3 |
| 32 | 26 | -11.98 | -12.43 | -12.26 | -12.06 |
| 34 | 28 | -12.71 | -13.18 | -12.94 | -12.77 |
| 36 | 29.8 | -13.42 | -13.9 | -13.66 | -13.45 |
| 38 | 31.7 | -14.1 | -14.56 | -14.3 | -14.1 |
| 40 | 39.5 | -14.75 | -15.24 | -14.95 | -14.78 |
| 42 | 39.8 | -15.42 | -15.9 | -15.63 | -15.46 |
| 44 | 39.8 | -16.1 | -16.52 | -16.3 | -16.14 |
| 45 | 37 | -16.39 | -16.82 | -16.6 | -16.74 |

Tab. 6 - Deflection increment- load data of GH2

| Displacement /mm | 0.1million Load/kN | 0.5million Load /kN | 1 million Load /kN | 1.5 million Load /kN | 2 million Load /kN |
|------------------|-----------------------|------------------------|-----------------------|-------------------------|-----------------------|
| 0 | -0.01 | 0 | 0 | 0 | 0 |
| 2 | -0.9 | -1.01 | -1.05 | -1.3 | 0.94 |
| 4 | -2.43 | -2.34 | -2.34 | -2.6 | 2.32 |
| 6 | -4 | -3.74 | -3.66 | -3.98 | 3.75 |
| 8 | -5.58 | -5.24 | -5.08 | -5.43 | 5.22 |
| 10 | -7.1 | -6.8 | -6.62 | -6.97 | 6.71 |
| 12 | -8.6 | -8.38 | -8.18 | -8.52 | 8.3 |
| 14 | -10 | -9.9 | -9.65 | -9.94 | 9.72 |
| 16 | -11.4 | -11.34 | -11.03 | -11.34 | 11.09 |
| 18 | -12.89 | -12.79 | -12.41 | -12.73 | 12.47 |
| 20 | -14.4 | 14.22 | -13.82 | -14.16 | 13.87 |
| 22 | -15.82 | -15.7 | -15.23 | -15.62 | 15.3 |
| 24 | -17.25 | -17.18 | -16.66 | -17.09 | 16.76 |
| 26 | -18.64 | -18.58 | -18.05 | -18.47 | 18.14 |
| 28 | -20.01 | -19.96 | -19.48 | -19.83 | 19.5 |
| 30 | -21.43 | -21.34 | -20.82 | -21.2 | 20.86 |
| 32 | -22.87 | -22.66 | -22.15 | -22.54 | 22.22 |
| 34 | -24.3 | -23.88 | -23.53 | -23.94 | 23.62 |
| 36 | -25.61 | -25.22 | -24.96 | -25.36 | 25.1 |
| 38 | -26.87 | -26.62 | -26.38 | -26.78 | 26.44 |
| 40 | -28.18 | -27.96 | -27.66 | -28.1 | 27.74 |
| 42 | -29.55 | -29.26 | -28.95 | -29.42 | 29 |
| 44 | -30.86 | -30.58 | -30.24 | -30.74 | 30.26 |
| 45 | -31.43 | -31.16 | -30.82 | -31.38 | 30.86 |

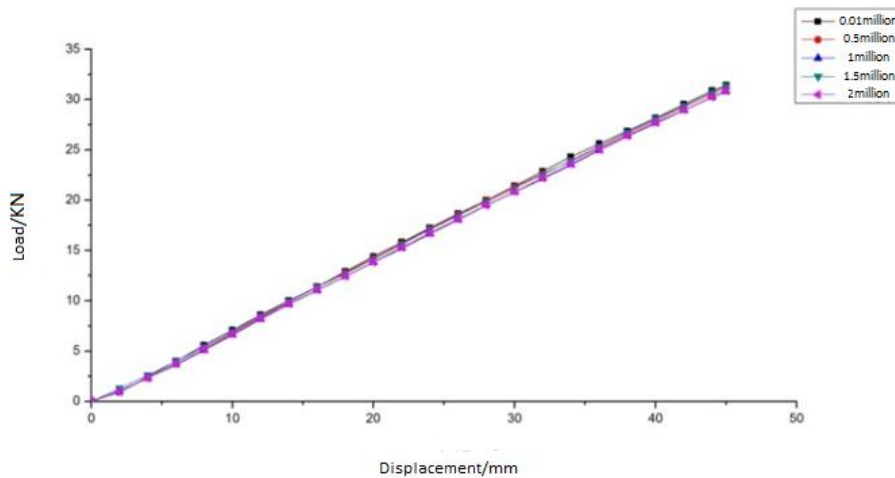


Fig. 10 - Deflection increment- load curve after different cycles loading

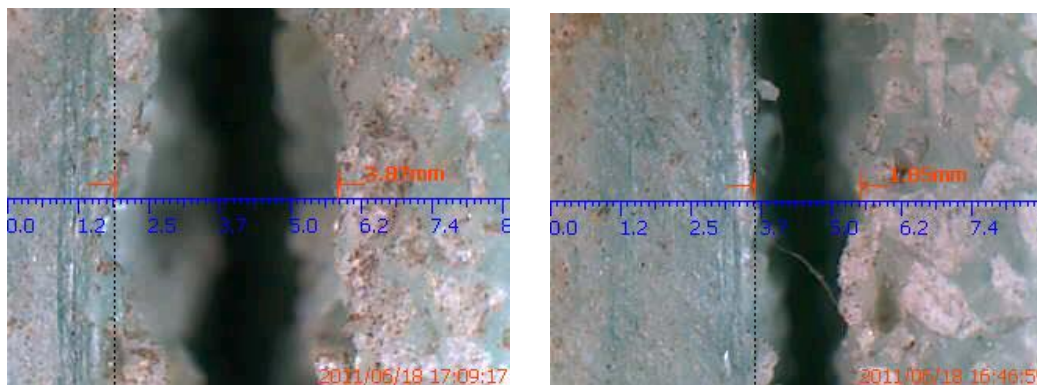


Fig. 11 - Width comparison of crack

The total number of the load is defined as the fatigue life when the specimen breaks completely. According to the Miner fatigue damage criterion, the fatigue life of FRPM can be characterized by the following equation:

$$R(n) = R_0 - \frac{n}{N}(R_0 - S_{\max}) \quad (4)$$

Where, $R(n)$ is the fatigue life after N times fatigue cycle, and R_0 is the initial ultimate strength; n is the number of times for the fatigue cycle, and N is the total number of fatigue cycles; S_{\max} is the stress level.

So a fatigue model which was shown in Equation 6 was used to analyse the fatigue property of FRPM. Fatigue parameters were obtained by the nonlinear regression method. The results were given in Table 9.

Based on the above experimental results of pipe culvert stress state of FRPM indoor fatigue test, it can be concluded that after 2.0 million times of fatigue, strength and stiffness of FRPM culvert were not significantly reduce, without layered peeling and brittle fracture phenomenon. According to the fatigue life prediction formula, its fatigue life completely meets to the requirements of the highway culvert application. This experiment and the further studies can be used widely in

highway culverts of FRPM and it provides a reliable basis of analysis in durability design.

CONCLUSION

In this paper, the mechanical performances of FRPM were investigated. The basic physical and mechanical properties of glass fiber reinforced plastic mortar pipe are analysed, and the technical requirements for the structural parameters, the basic mechanical indexes and durability characteristics of FRPM pipe are analysed. The following conclusions can be drawn.

Resin and quartz sand composite improve compression resistance of FRPM significantly, and the relationship between compression resistance property and loading is linear. The ring and axial elastic modulus is 4.84 GPa, and 3.04 GPa respectively. The influence of quartz sand on compressive resistance property is more significant than glass fiber and resin.

Though parallel plate performance test under external load, the load - deformation relationship were measured and pipe stiffness (PS) is obtained.

The long term performance of FRPM pipes after 2 million fatigue load is degraded up to 25% of the initial performance. Although the ultimate bearing capacity of glass fiber reinforced plastic sand pipe under fatigue loading decreases, the failure form has the trend from brittle to plasticity.

In summary, the culverts constructed with FRPM have a better mechanics and durability performance than those with the concrete. This experiment and the following research provide a reliable basis for the design of FRPM pipe in the application of highway culvert. A trial section of FRPM should be put into effect in the future in order to determine the applicability for different regions.

REFERENCES

- [1] Arjomandi K, Taheri F. (2011). "A new look at the external pressure capacity of sandwich pipes." *Marine Structures*, Vol. 24, No. 24, pp. 23-42, DOI: 10.1016/j.marstruc.2010.12.001.
- [2] Farshad M., Necola A. (2004). "Effect of aqueous environment on the long-term behavior of glass fiber-reinforced plastic pipes." *Polymer Testing*, Vol. 23, No. 2, pp. 163-167, DOI:10.1016/S0142-9418(03)00075-8.
- [3] Gargiulo C, Marehetti M, Rizzo A. (1996). "Prediction of failure envelopes of composite tubes subjected to biaxial loadings." *Acta Astronautica*, Vol. 39, No. 5, pp. 355-368, DOI:10.1016/S0094-5765(96)00081-1.
- [4] Guo Q L, Bian Y S, Li L L, Jiao Y B, Tao J L, Xiang C X. (2015). "Stereological estimation of aggregate gradation using digital image of asphalt mixture." *Construction and Building Materials*, Vol. 94, pp. 458-466, DOI:10.1016/j.conbuildmat.2015.07.046.
- [5] Jeyapalan J K, Thiyagaram M, Saleira W E, et al. (1989). "Analysis and design of RPM and other composite underground pipelines." *Journal of Transportation Engineering*, Vol. 115, No. 3, pp. 219-231, DOI:10.1061/(asce)0733-947x(1989)115:3(219).
- [6] Kaynak C, Erdiller E S, Parnas L, et al. (2005). "Use of split-disk tests for the process parameters of filament wound epoxy composite tubes." *Polymer Testing*, Vol. 24, No. 24, pp. 648-655, DOI:10.1016/j.polymertesting.2005.03.012.
- [7] Li Y S, Feng W J, Cai Z Y. (2014). "Bending and free vibration of functionally graded piezoelectric beam based on modified strain gradient theory." *Composite Structures*, Vol. 115, pp. 41-50, DOI: 10.1016/j.compstruct.2014.04.005.

- [8] Ouellette H, Beach L. (1981) . "Rehabilitation of sanitary sewer pipelines." *Transportation Engineering Journal of ASCE*, Vol. 107, No. 4, pp. 497-513.
- [9] Qi H Y, Wen W D. (2001) . "Progress in research on fiber-reinforced composite fatigue." *Materials Reviews*, Vol. 15, No. 1, pp. 36-38.
- [10] Rafiee R, Amini A. (2015). "Modeling and experimental evaluation of functional failure pressures in glass fiber reinforced polyester pipe." *Computational Materials Science*, Vol. 9, pp. 579-588, DOI:10.1016/j.commatsci.2014.03.036.
- [11] Rafiee R, Reshadi F. (2014) . "Simulation of functional failure in GRP mortar pipes." *Composite Structures*, Vol. 113, No. 1, pp. 155-163, DOI: 10.1016/j.compstruct.2014.03.024.
- [12] Roy A K, Tsai S W. (2012) . "Three-Dimensional effective module of orthotropic and symmetric laminates." *Journal of Applied Mechanics*, Vol. 59, No. 1, pp. 39-47, DOI:10.1115/1.2899462.
- [13] Sung H Y, Jin O O. (2015) . "Prediction of long term performance for GRP pipes under sustained internal pressure." *Composite Structures*, Vol. 134, pp. 185-189, DOI:10.1016/j.compstruct.2015.08.075.
- [14] Xia M, Takayanagi H, Kemmochi K. (2001) . "Analysis of multi-layered filament-wound composite pipes under internal pressure." *Composite Structures*, Vol. 53, No. 4, pp. 483-491, DOI:10.1016/S0263-8223(01)00061-7.
- [15] Xu Ying, Wen W D, Cui H P. (2006) . "A cumulative damage prediction method of low velocity impacts on laminated composites." *Journal of Materials Science and Engineering*, Vol. 24, No. 1, pp. 77-81.